Germline genetics, disease, and exposure to medication influence longitudinal dynamics of clonal hematopoiesis

Clonal hematopoiesis of indeterminate potential (CHIP) occurs when a hematopoietic stem cell acquires a somatic driver mutation in a leukemia-associated gene, with a variant allele fraction (VAF) exceeding 2% in peripheral blood.[1] Higher VAF is associated with increased morbidity and mortality risk.[2-5] Identifying factors influencing clonal expansion rate is crucial for risk stratification in CHIP patients. Recent cost-effective targeted assays have enabled serial sequencing and longitudinal profiling of CHIP dynamics.[6] We present the largest longitudinal analysis of CHIP mutational dynamics to-date, examining 3,000 individuals from the Vanderbilt BioVU biobank. Our findings reveal that CHIP growth rates vary significantly by driver gene and are influenced by germline variants and medication exposures. Additionally, we demonstrate that monitoring blood counts may be more informative for risk stratification than frequent resequencing in CHIP patients.

We performed targeted, error-corrected sequencing on serial blood samples from 3,000 individuals in the Vanderbilt BioVU biobank, using custom-designed probes for 22 CHIP-associated genes (*Online Supplementary Table S1*; *Online Supplementary Figure S1*). Vanderbilt University Medical Center's Institutional Review Board oversees BioVU and approved this project (IRB #201783). Unique molecular identifiers (UMI) were used for error correction, excluding mutations detected from a single UMI. The mean coverage depth was 1,725x after de-duplication. CHIP mutations were called for variants with ≥100x total read depth, ≥3 variant allele reads, and >2% VAF in at least one blood draw. We identified 893 CHIP mutations in 711 individuals (Figure 1A). Participants' mean age at first draw was 70 years (range, 19-96), with a mean 5.7-year interval (range, 0.7-13) between samples. Mean VAF were 6.7% and 9.5% at first and second draws, respectively. Most individuals (79%) had a single CHIP mutation, 16% had two, and 4% had three or more (Figure 1B). *DNMT3A* and *TET2* were the most frequently mutated genes. Of the 711 individuals, 74% had CHIP at both time points, while 26% had >2% VAF at only one draw, predominantly (78%) at the second draw.

We modeled the growth rate *r* with a compound interest formula $r = \frac{VAF_2}{VAF_1}^{1/time}$ -1. *SRSF2/SF3B1* (splicing factor) driver mutations exhibited the fastest average growth rate (~25% annually), while *DNMT3A* driver mutations showed the slowest rate (~7% annually) (Figure 1C). Seventy-eight percent of mutations increased in VAF (annual growth rate >1%), consistent with prior studies.[5,7] Decreases in VAF (annual growth rate <-1%) were observed in 30% of *JAK2*, 21% of *ASXL1*, 25% of *DNMT3A*, 19% of *PPM1D*, 19% of *TET2*, and 0% of *SRSF2/SF3B1* mutations. While certain driver genes were more prone to expansion, CHIP expansion rates varied considerably among individuals with the same driver gene. This variability may necessitate larger sample sizes in prospective randomized controlled trials aiming to identify drugs that slow expansion.

We analyzed individuals with two CHIP mutations, which may co-occur as subclones or in distinct cells (Figure 1D). Mutation pairs were classified as subclones if their growth rates were within 0.6 standard deviations of each other; otherwise, they were considered distinct. Of 116 individuals with two mutations, 66 (57%) pairs were subclones. Subclones showed significantly lower growth rates than distinct clones (β=-0.15, *P*=0.02) (Figure 1E). This finding was robust for standard deviation thresholds from 0.4 to 0.8. Co-occurrence analysis of CHIP mutations by driver gene (Figure 1F) revealed that *JAK2* and *SF3B1/SRSF2* co-occurred significantly more often than expected (odds ratio [OR]=48.7, *P*=0.0006). Two mutations in *TET2* (OR=6.6, *P*=0.001), *DNMT3A* (OR=3.8, *P*=0.006), and *PPM1D* (OR=8.7, *P*=0.02) also occurred more frequently than chance. Conversely, *DNMT3A* and *TET2* co-occurred less often than expected based on frequency (OR=0.4, *P*=0.02) (Figure 1G).

We investigated individual determinants of CHIP expansion rate. When accounting for driver gene mutations, growth rate showed no significant association with age (*P*=0.07), body mass index (*P*=0.68), biological sex (*P*=0.89), or smoking status (*P*=0.70). Our targeting assay included probes for germline variants previously linked to CHIP prevalence and estimated growth rate (Figure 2A).[1,8] Each additional G allele in rs1800057 (ATM) correlated with increased growth rate (β=0.46, 95% confidence interval [CI]: 0.23 to 0.67, *P*<0.001; Figure 2B), potentially explaining its association with CHIP prevalence.[1] Consistent with NHLBI's TOPMed cohort findings,[9] each T allele at rs2887399 (in the *TCL1A* promoter) associated with increased *DNMT3A* expansion rate (*P*=0.04) and decreased *TET2* expansion rate (*P*=0.02) (Figure 2C).

We investigated associations between medication exposure duration and CHIP growth rate. While no medications showed significant associations after multiple hypothesis correction, several demonstrated suggestive effects (Figure 2D). Exposure to three drugs suggested reduced annual growth rates: colchicine (β=-3.5%, 95% CI: -0.5 to -7, *P*=0.03), denosumab (β=-2.5%, 95% CI: -0.3 to -5, *P*=0.03), and methylprednisolone (β=-1.0%, 95% CI: -0.4 to -2, *P*=0.01). These associations have biological plausi-

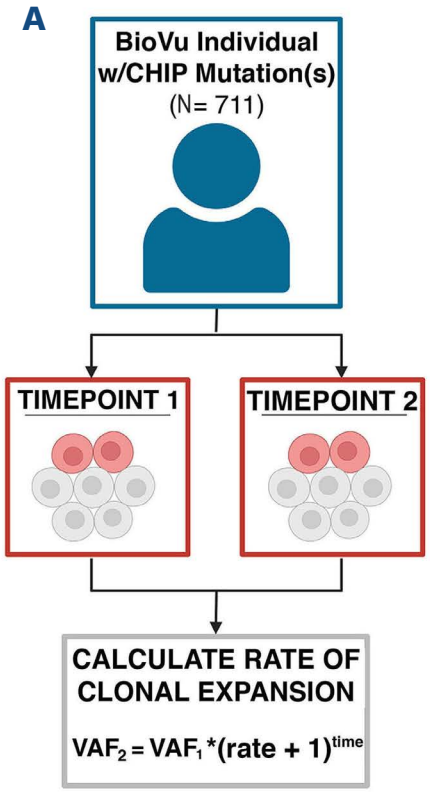

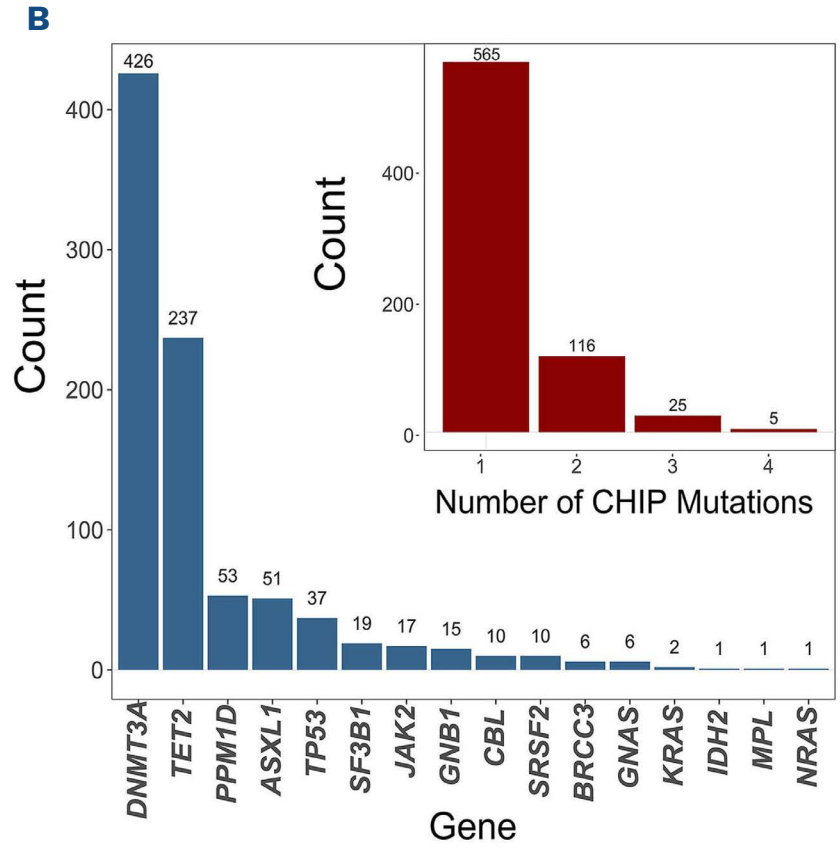

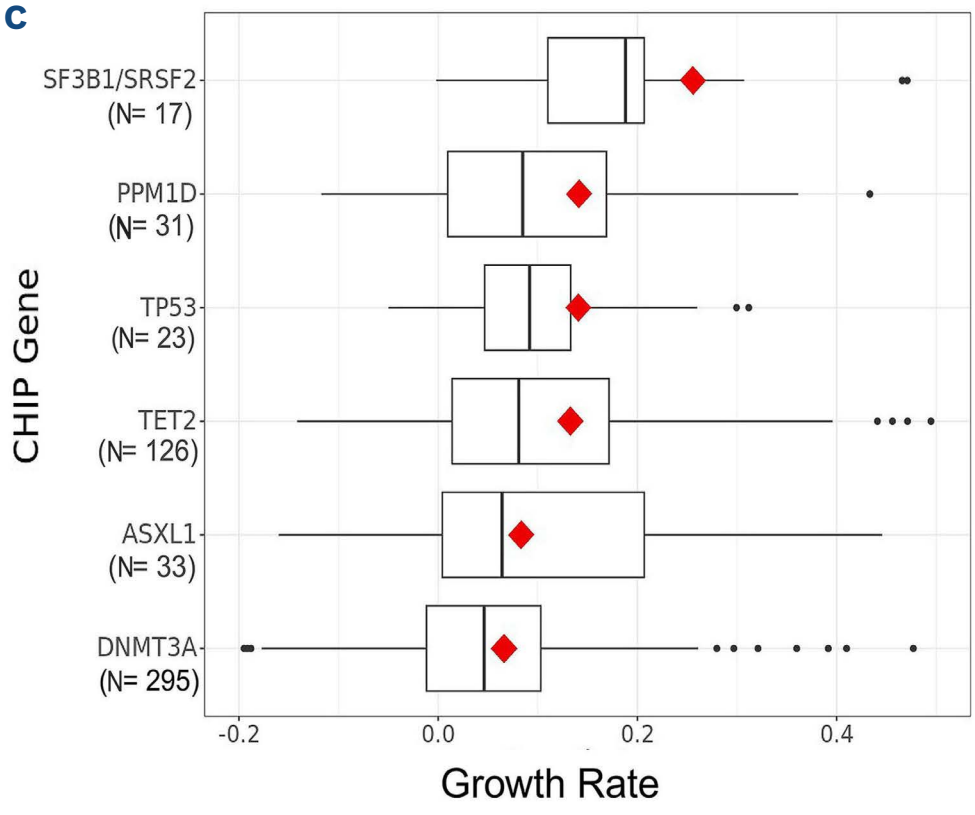

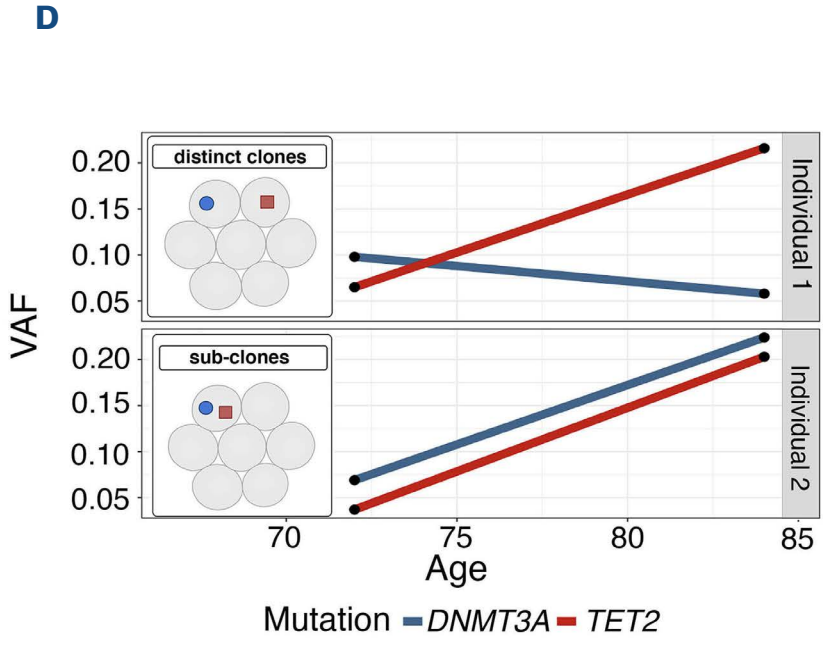

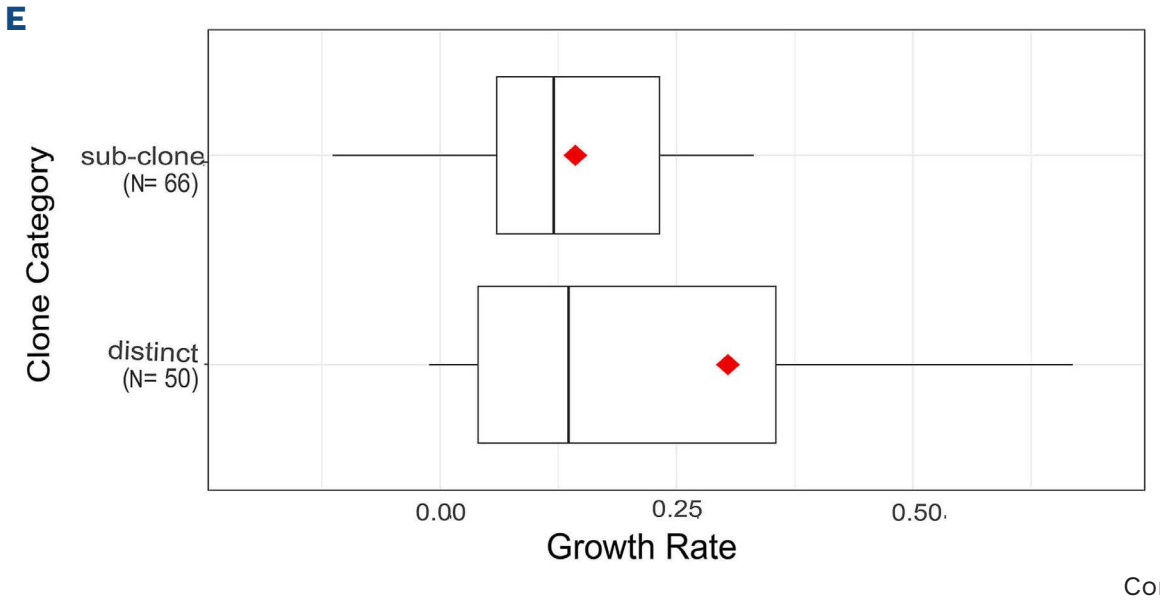

Continued on following page.

F

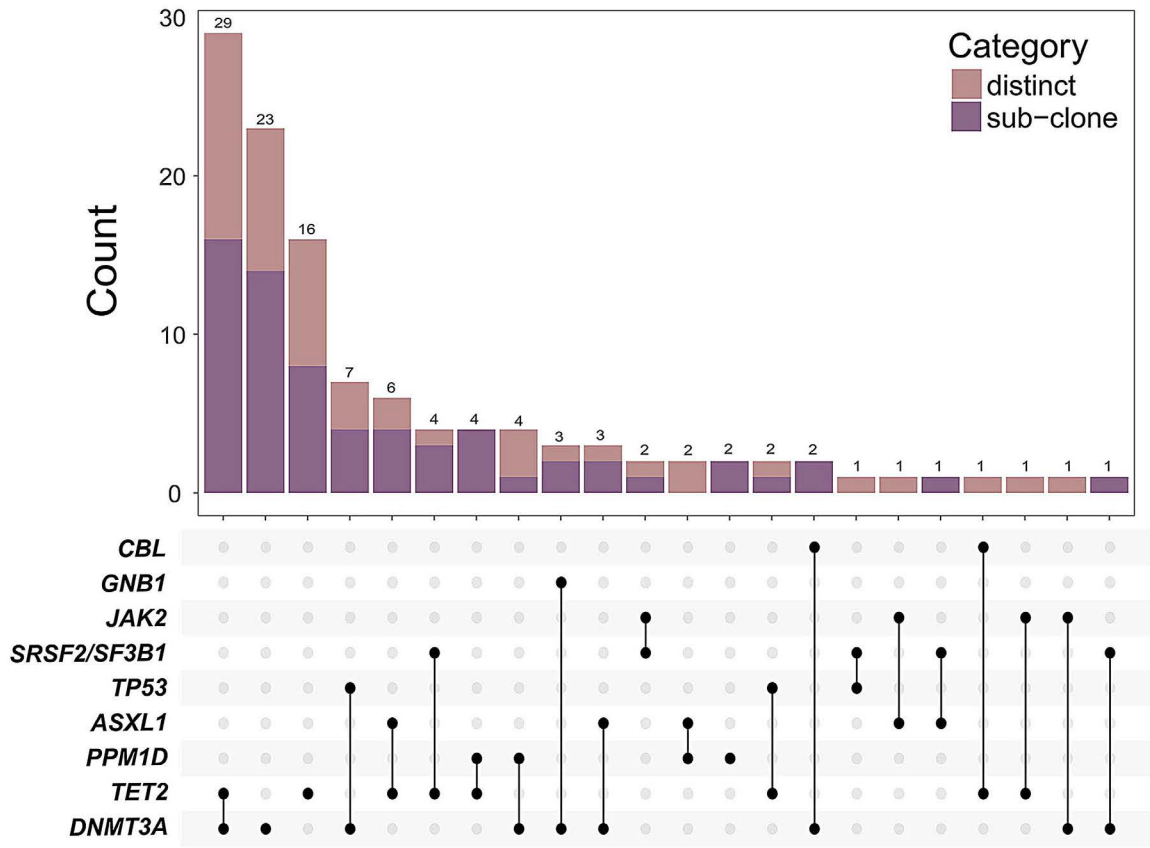

G

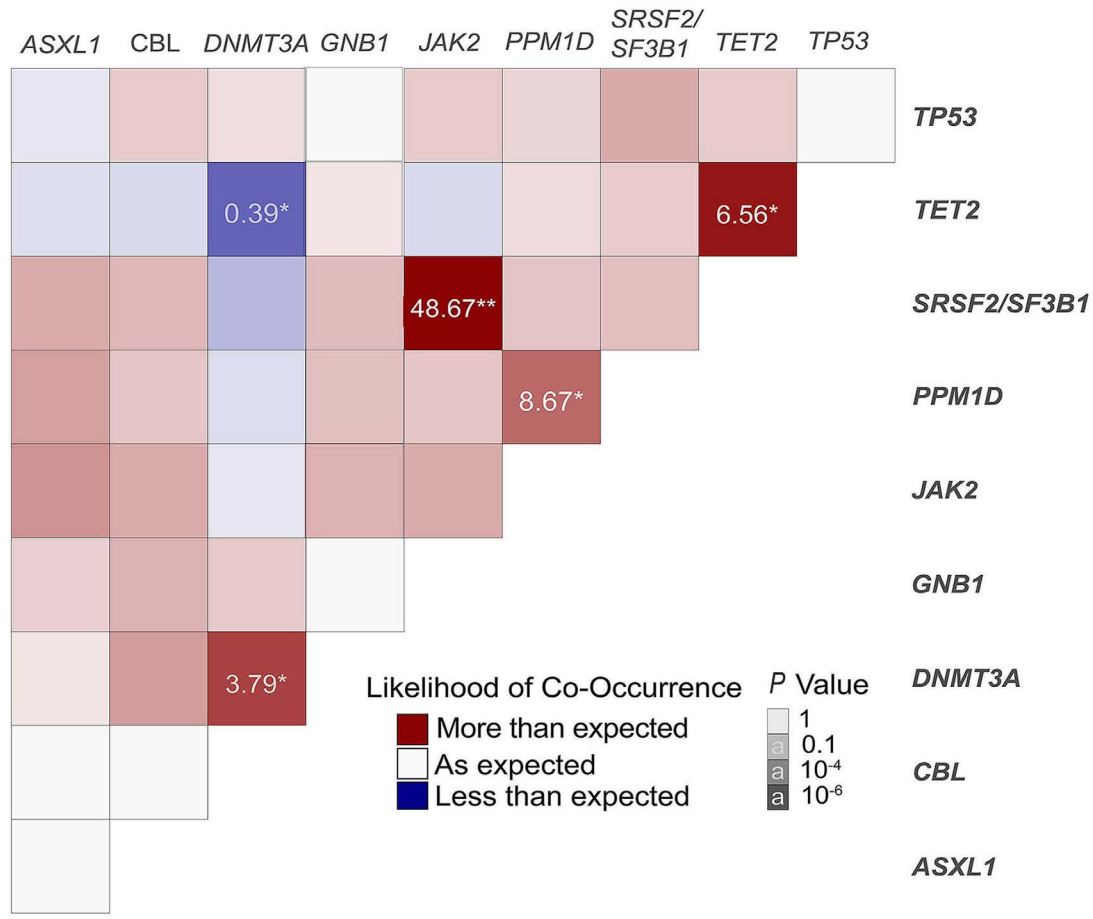

Figure 1. Cohort characteristics and co-occurring clonal hematopoiesis of indeterminate potential mutations. (A) Our cohort consists of 892 clonal hematopoiesis of indeterminate potential (CHIP) mutations in 711 individuals. We calculated growth rate using a compound interest formula for sequencing at 2 blood draws. (B) Larger bar plot demonstrates the number of CHIP with a mutation in a driver gene. Smaller bar plot shows the number of individuals with 1, 2, 3, and 4 CHIP mutations. (C) Box plot of growth rate, calculated with a compound interest formula, for each CHIP mutation by driver gene with number of individuals with mutations in the driver gene shown below the gene name. Red diamond represents the mean growth rate. Box represents the interquartile range of the growth rate. Middle line in the box represents the median of the growth rate. (D) Theoretical example of possible trajectories for individuals with two CHIP mutations. The mutations can either be in distinct cell populations or the same cell population. Variant allele fraction (VAF) trajectories for each of these scenarios should fol-

Continued on following page.

low similar trends to this example. Each mutation is represented by color, and the line represents change in VAF between first and second blood draws. (E) Box plot showing the difference in average growth rate of the fastest growing mutations for the 116 individuals grouped into the distinct *versus* sub-clone categories. The red diamond represents the average of the growth rate. Box represents the interquartile range of the growth rate. Middle line in the box represents the median of the growth rate. The x-axis is the growth rate while the y-axis is the category. (F) Upset plot showing the different combinations of driver genes represented within the group of 116 individuals with multiple CHIP mutations. Above the upset plot is a bar plot showing the distribution between distinct *versus* sub-clone trajectories for each of the driver gene combinations, with driver gene on the x-axis and count on the y-axis. (G) Heat map showing the deviation from random for the co-occurrence of each driver gene pair for the 116 individuals with 2 CHIP mutations. Each gene pair was tested with a Fisher's exact test to identify deviation from expected occurrence via random chance. The x- and y-axes represent each gene in a pair, the color of the box represents the direction of the deviation from random, and the darkness of the hue represents the magnitude of the deviation. For gene combinations with a *P* value >0.05, the odds ratio is displayed, and the box is marked with "*" and for gene combinations that passed multiple-hypothesis correction with a *P* value of <0.001, the odds ratio is displayed and the box is marked with "**".

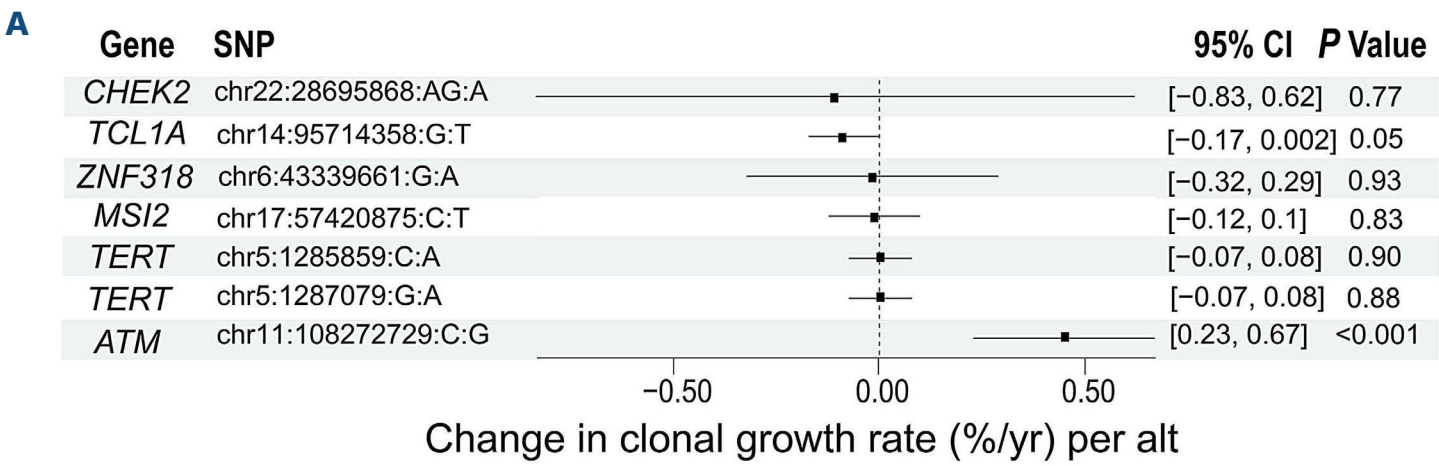

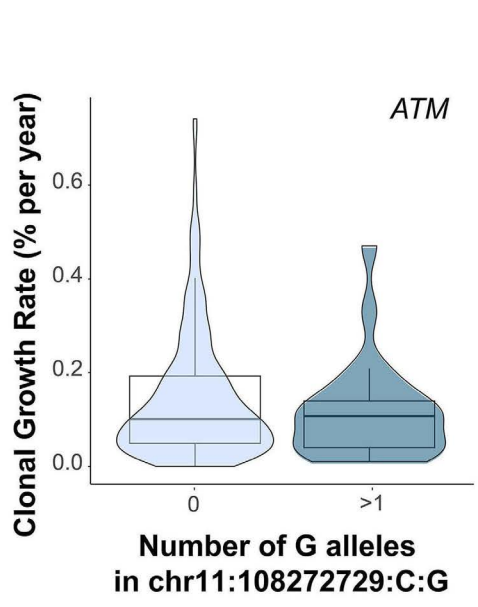

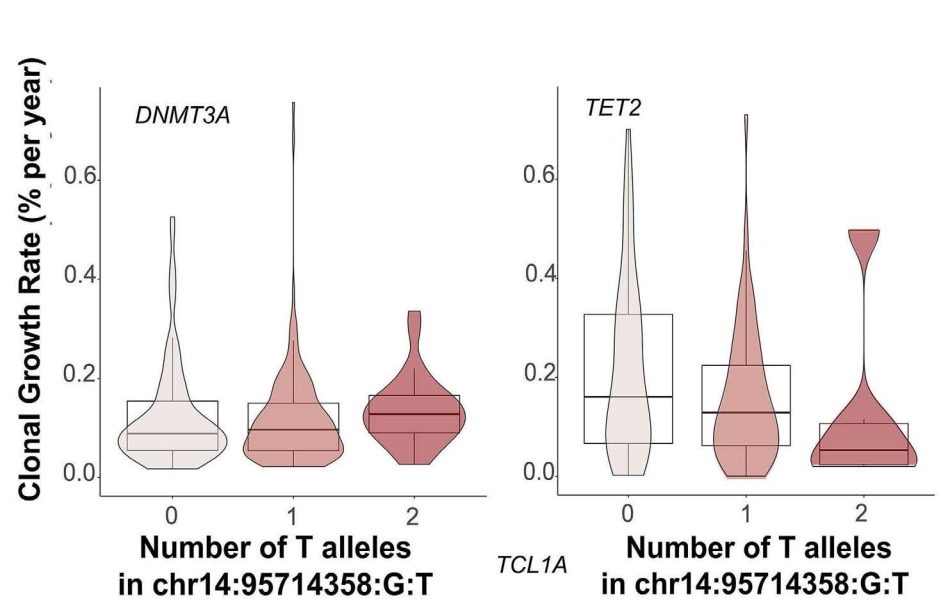

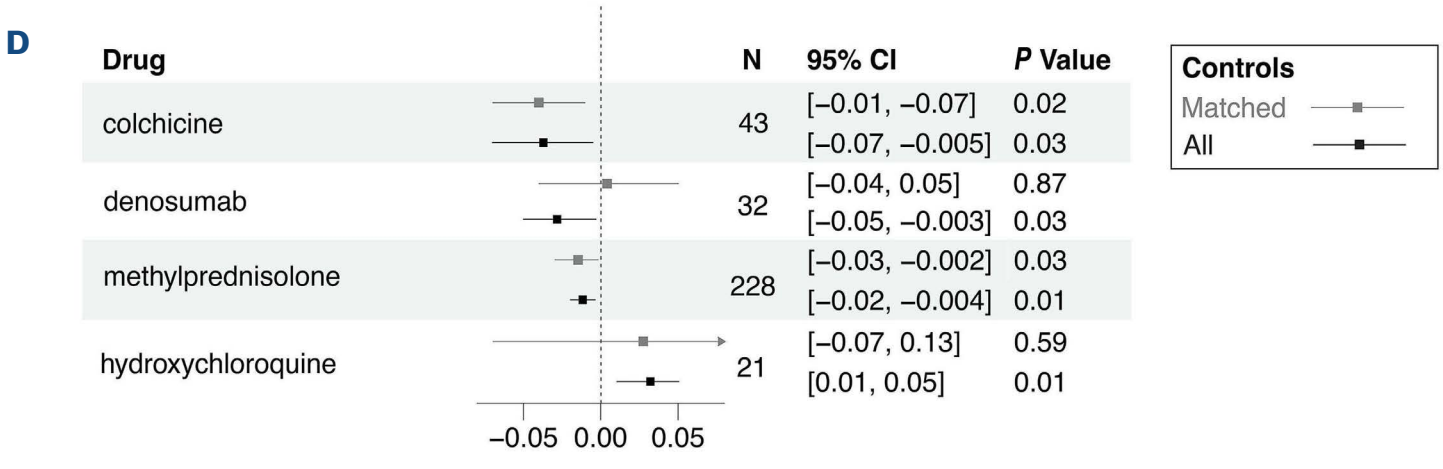

Continued on following page.

E

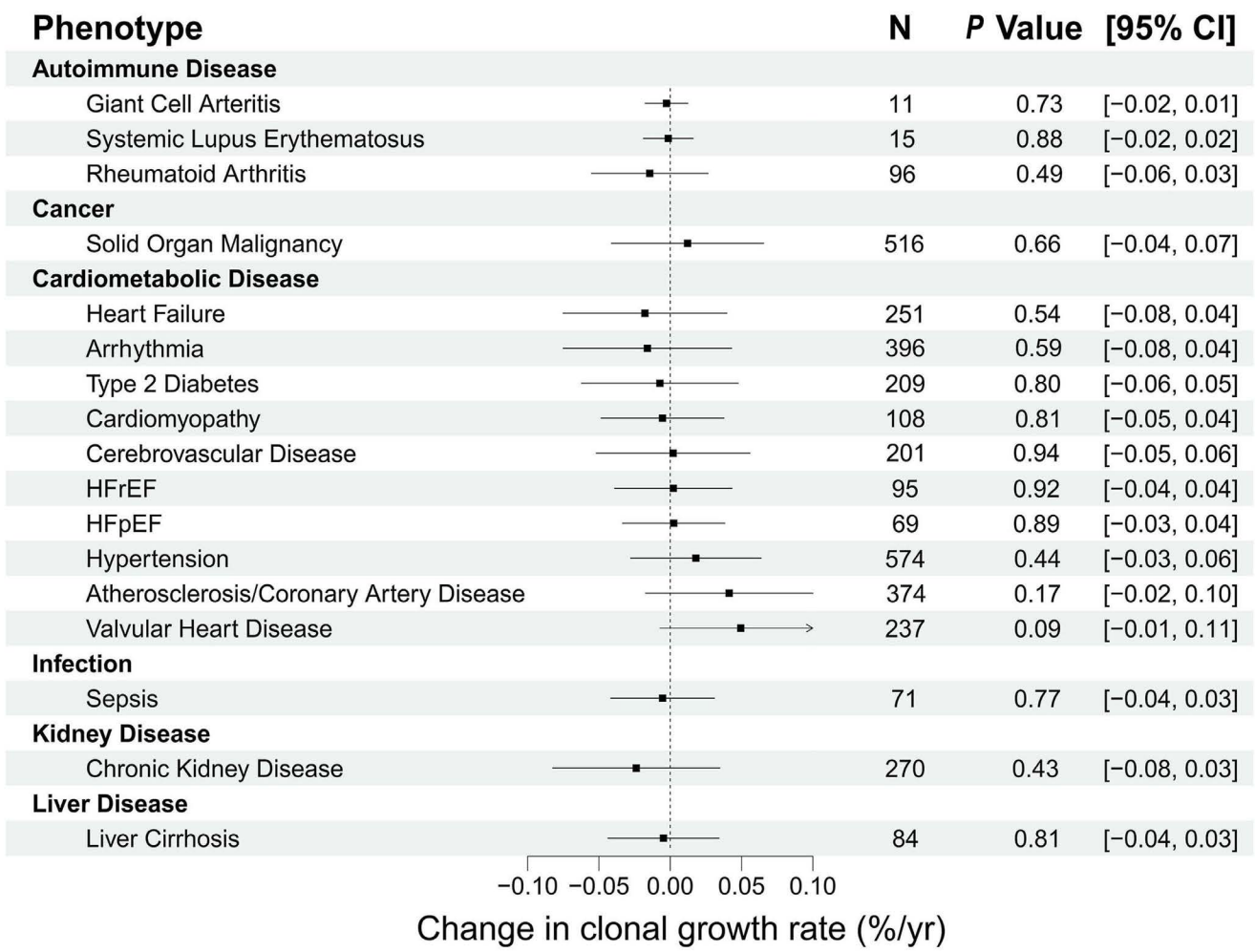

Figure 2. Determinants of clonal hematopoiesis of indeterminate potential growth rate. (A) Forest plot of change in annual growth rate (%/yr) with each additional copy of the alternate allele (alt) for select germline single nucleotide polymorphisms (SNP) detectable with the targeted sequencing assay among individuals with clonal hematopoiesis of indeterminate potential (CHIP) mutations. Effect estimate represents the coefficient of a linear regression of growth rate and number of alternate alleles modeled additively as 0, 1, or 2, adjusting for age, sex, race, and variant allele fraction (VAF) at first sequencing. We computed the 95% confidence interval (95% CI) as the effect estimate +/- 1.96 standard error. The *P* value tests the null hypothesis of the effect estimate being 0. (B) Violin plot of %/yr for 0 *versus* >1 G allele for germline variant chr11:108272729:C:G in *ATM*. When modeled additively, each additional G allele is associated with greater %/yr in multiple linear regression by 0.46% per year (95% CI: 0.23-0.67, *P*<0.001). There were 619 CHIP mutations in individuals with 0 G alleles, 26 in individuals with 1 G allele, and 2 in individuals with 2 G alleles. (C) Violin plot of %/yr for 0, 1, and 2 T alleles for germline variant chr14:95714358:G:T in TCL1A for *DNMT3A* CHIP (left) and *TET2* CHIP (right). When modeled additively, each additional T allele is associated with greater %/yr for *TET2* CHIP mutations (*P*=0.03), but not for *DNMT3A* CHIP mutations (*P*=0.49). There were 132 *TET2* mutations in individuals with 0 T alleles, 54 *TET2* mutations in individuals with 1 T allele, and 6 *TET2* mutations with 2 T alleles. There were 158 *DNMT3A* mutations in individuals with 0 T alleles, 95 *DNMT3A* mutations in individuals with 1 T allele, and 28 *DNMT3A* mutations in individuals with 2 T alleles. (D) Forest plot of change in annual growth rate (%/yr) with each additional prescription month of 4 selected drugs with suggestive associations: colchicine, denosumab, methylprednisolone, and hydroxychloroquine. Black effect estimate represents the coefficient of a linear regression of growth rate and number of months exposed to the drug adjusting for age, sex, race, and VAF at first sequencing with all data. Gray effect estimate represents the coefficient of a linear regression of growth rate and number of months exposed to the drug for 3:1 matched non-drug-exposed controls to drug-exposed cases (matched by age, sex, CHIP driver gene, VAF at first sequencing). We computed the 95% CI as the effect estimate +/- 1.96 standard error. The *P* value tests the null hypothesis of the effect estimate being 0. N represents the number of individuals prescribed the drug for at least 1 month. (E) Forest plot of change in %/yr among individuals with select pre-existing diagnoses based on phecodes. Individuals had to have their first diagnosis of the phecode before their second blood draw. Estimate represents the coefficient of a linear regression of growth rate and presence of diagnosis as a binary variable adjusting for age, sex, race, and VAF at first sequencing. We computed the 95% CI as the effect estimate +/- 1.96 standard error. The *P* value tests the null hypothesis of the effect estimate being 0. N represents the number of individuals with the diagnosis in each regression.

bility: methylprednisolone has anti-inflammatory effects, colchicine may abrogate cardiovascular risk in *TET2* CHIP, and denosumab inhibits *RANKL*, which *DNMT3A*-mutated monocytes overexpress in bone.[10] Conversely, hydroxychloroquine suggested increased annual growth rate (β=3.1%, 95% CI: 0.3-5, *P*=0.03). Moreover, we performed 3:1 case-control matching by age, sex, CHIP driver gene, baseline VAF, and drug indication for each drug and tested the association with growth rate. In this sensitivity analysis, we still observed an association between exposure duration between sequencing time points of colchicine and methylprednisolone and decreased growth

A

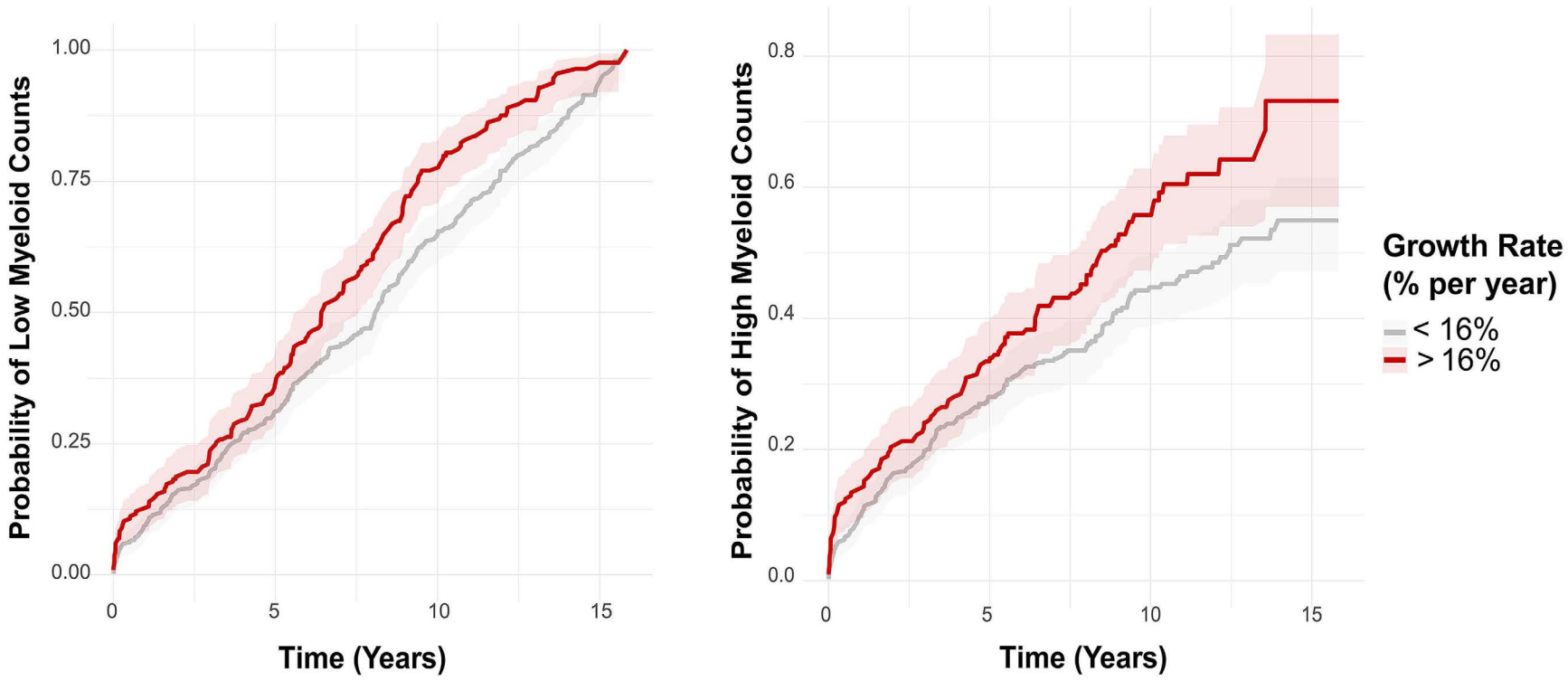

B

Phenotype	N Individuals	*P* Value	[95% CI]
Cancer			
Myeloproliferative Disease	23	0.02	[0.10, 0.92]
Cardiovascular Disease			
Cerebrovascular Disease	48	0.89	[−0.32, 0.27]
Valvular Heart Disease	209	0.97	[−0.14, 0.14]
Arrhythmia	135	0.39	[−0.10, 0.25]
Cardiomyopathy	35	0.47	[−0.21, 0.45]
Atherosclerosis/Coronary Artery Disease	145	0.1	[−0.03, 0.31]
Hypertension	33	0.36	[−0.19, 0.51]
Heart Failure	42	0.22	[−0.12, 0.50]
Infection			
Sepsis	37	0.98	[−0.34, 0.33]
Kidney Disease			
Chronic Kidney Disease	70	0.66	[−0.19, 0.30]
Mortality			
Death	99	0.94	[−0.21, 0.20]

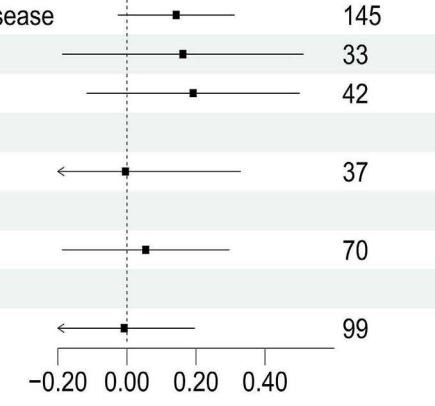

C

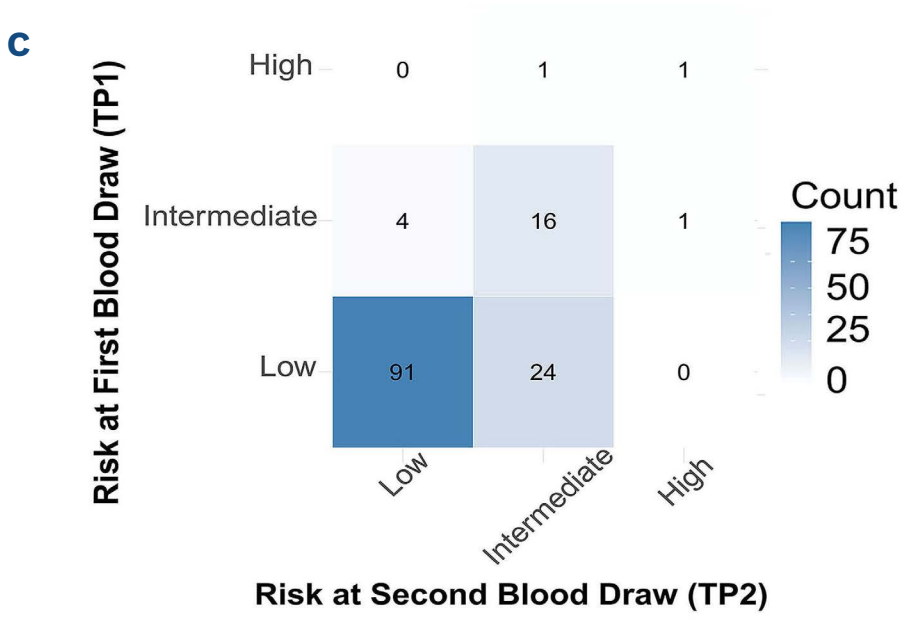

Continued on following page.

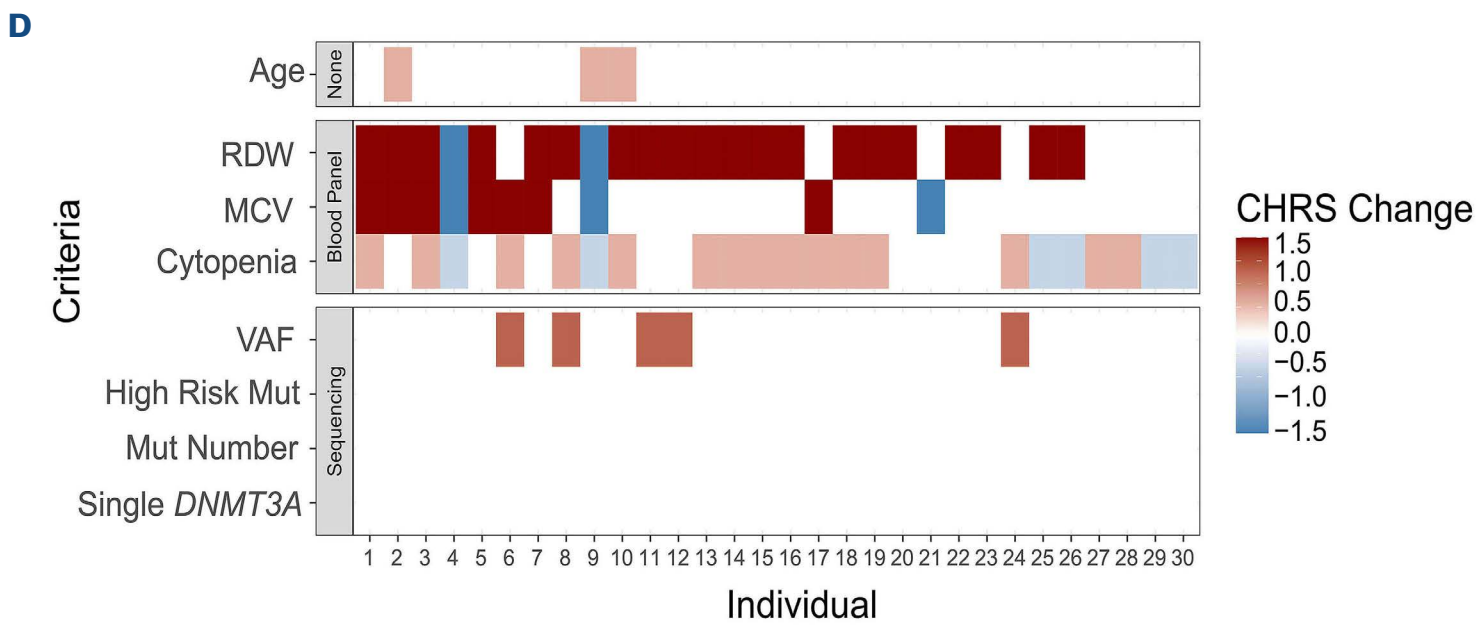

Figure 3. Phenotypic consequences of growth rate. (A) On the left, Kaplan-Meier curve of time to low myeloid counts - defined as thrombocytopenia (platelet count <169.06x10^9 cells/L), anemia (red blood cell count <3.96x10^{12} cells/L) or neutropenia (neutrophil count <1.47x10^9 cells/L) for individuals with a CHIP growth rate >16% annually (red) and <16% annually (gray). A Cox proportional hazard model of time to low myeloid counts and rank-inverse normalized growth rate, when adjusting for age, variant allele fraction (VAF) at the first blood draw, and sex was significant (hazard ratio [HR]=1.20, 95% confidence interval [CI]: 1.05-1.36, *P*<0.001). On the right, Kaplan-Meier curve of time to high myeloid counts - defined as thrombocytosis (platelet count >397.1x10^9 cells/L), polycythemia (red blood cell count >5.5x10^{12} cells/L), or elevated neutrophil count (neutrophil count >7.06x10^9 cells/L) for individuals with a clonal hematopoiesis of indeterminate potential (CHIP) growth rate >16% annually (red) and <16% annually (gray). A Cox proportional hazard model of time to high myeloid counts and rank-inverse normalized growth rate, when adjusting for age, VAF at the first blood draw, and sex was significant (HR=1.14, 95% CI: 1.02-1.27, *P*=0.003). (B) Forest plot showing the association between growth rate and time to event for the listed phenotypes. Out of the 711 individuals in the study, individuals who had a phenotype for the first time after the second blood draw are included, with each phenotype sample size listed in the figure. (C) Heatmap showing Clonal Hematopoiesis Risk Score (CHRS) category at the first blood draw (TP1) *versus* risk at second blood draw (TP2) for N=134 individuals with data available to compute a CHRS (blood counts, mean corpuscular volume, and red cell distribution width). As per Weeks *et al.*[43], low risk was defined as CHRS ≤9.5, intermediate risk as 10< CHRS <12, and high risk as CHRS ≥12.5. Darker hues represent higher numbers of individuals, and exact counts are displayed for each category. (D) Heatmap showing the change in each of the CHRS criteria for the N=30 individuals that shifted into a different risk category between first and second blood draw. The x-axis represents each individual and the y-axis represents the CHRS components, which are faceted based on what clinical test would need to be performed to ascertain that information (i.e., none, blood panel, and sequencing). The color of the box represents the direction of the change (red is positive and blue is negative) and the darkness of the hue represents the magnitude of the change.

rate. In external validation cohort Clonal Hematopoiesis and Inflammation in the Vasculature (CHIVE)[11], four of five mutations exposed to colchicine and eight of ten exposed to methylprednisolone demonstrated reduced or unchanged VAF (*Online Supplementary Figure S2*). We found no associations between pre-existing diagnoses and CHIP expansion rate (Figure 2E). The lack of association between pre-existing atherosclerosis and CHIP growth rate supports a unidirectional association between clonal hematopoiesis and atherosclerosis.[12]

We investigated the consequences of CHIP expansion rate on blood counts and diagnoses after the second blood draw. Analyzing associations between growth rate and time to blood cell count abnormalities (as defined in Niroula *et al.*[13]), we found that rank-inverse normalized growth rate, adjusted for age, baseline VAF, and sex, was associated with shorter time to high myeloid cell parameters (hazard ratio [HR]=1.14, 95% CI: 1.02-1.27) and low myeloid cell parameters (HR=1.20, 95% CI: 1.05-1.36). No associations were found with lymphocytosis (*P*=0.48) or lymphopenia (*P*=0.53). Annual growth rate >16% increased risk of both high and low myeloid cell parameters (*P*=0.003 and *P*<0.001, respectively) (Figure 3A). A 1% increase in annual growth rate suggested a 1.6-fold increased risk of myeloproliferative disorders (95% CI: 1.1-2.5, *P*=0.02), though this association was not significant after multiple-hypothesis correction (Figure 3B). These findings indicate that faster growth rate heightens disease risk in individuals with CHIP.

We next examined changes in clinical risk scores over time, focusing on the Clonal Hematopoiesis Risk Score (CHRS) for 138 individuals with complete blood count data within 6 months of sequencing.[14] Of 115 individuals initially classified as low risk (CHRS ≤9.5), 24 (21%) were reclassified as intermediate risk (10< CHRS <12) at the second blood draw (Figure 3C). Among 21 initially intermediate-risk individuals, four (19%) were reclassified as low risk, and one (5%) as high risk (CHRS ≥12.5). Only two individuals were classified as high risk overall. Risk category changes were primarily driven by alterations in blood counts (Figure 3D). Every individual who shifted CHRS category had new alterations in RDW, MCV, or blood counts. Only five (17%) exceeded the 20% VAF threshold, but all five also had blood count changes. These

findings suggest that repeated blood sequencing may be unnecessary without accompanying laboratory abnormalities. Our study has notable limitations. Despite being the largest cohort of longitudinal CHIP clonal dynamics to-date, we lack power to detect clinical consequences of CHIP growth rate due to the short follow-up time and low-risk population. The exclusion of individuals with hematologic malignancies further limits our ability to detect associations between CHIP growth rate and these phenotypes. Additionally, associations between medication exposure and growth rate are susceptible to confounding by indication, although we observed no associations between pre-existing diagnoses and growth rate for the medications of interest and colchicine and methylprednisolone had a significant negative association in matched controls.

In conclusion, we present the largest longitudinal study of CHIP dynamics to date. Our findings demonstrate that germline genetics, medications, driver genes, and mutation numbers significantly influence CHIP growth rates, with considerable individual variation. As targeted CHIP panels become more accessible, clinicians may leverage these identified risk factors and CHIP trajectories to better assess clinical risk in individuals with CHIP.

Authors

Taralynn Mack,[1*] Yash Pershad,[1*] Caitlyn Vlasschaert,[2] Cosmin A. Bejan,[3] Jonathan Brett Heimlich,[4] Yajing Li,[5,6] Nicole A. Mickels,[1] Joseph C. Van Amburg,[1] Jessica Ulloa,[1] Alexander J. Silver,[4,7] Leo Y. Luo,[8] Angela Jones,[1] Paul Brent Ferrell,[9] Ashwin Kishtagari,[4,10] Yaomin Xu,[5,6] Michael R. Savona[4,7,10,11] and Alexander G. Bick[1,12]

[1]Vanderbilt Genetics Institute, Vanderbilt University, Nashville, TN, USA; [2]Department of Medicine, Queen's University, Kingston, Ontario, Canada; [3]Department of Biomedical Informatics, Vanderbilt University Medical Center, Nashville, TN, USA; [4]Department of Medicine, Vanderbilt University Medical Center, Nashville, TN, USA; [5]Department of Biomedical Informatics, Vanderbilt University Medical Center, Nashville, TN, USA; [6]Department of Biostatistics, Vanderbilt University Medical Center, Nashville, TN, USA; [7]Program in Cancer Biology, Vanderbilt University School of Medicine, Nashville, TN, USA; [8]Department of Radiation Oncology, Vanderbilt University Medical Center, Nashville, TN, USA; [9]Division of Hematology and Oncology, Department of Medicine, Vanderbilt University Medical Center, Nashville, TN, USA; [10]Vanderbilt Ingram Cancer Center, Vanderbilt University Medical Center, Nashville, TN, USA; [11]Center for Immunobiology, Vanderbilt University Medical Center, Nashville, TN, USA and [12]Division of Genetic Medicine, Vanderbilt University Medical Center, Nashville, TN, USA

**TM and YP contributed equally as first authors.*

Correspondence:
A. BICK - alexander.bick@vumc.org

https://doi.org/10.3324/haematol.2024.286513

Received: August 22, 2024.
Accepted: November 6, 2024.
Early view: November 14, 2024.

Disclosures

AGB has received honoraria for advisory board membership from, and holds equity in TenSixteen Bio. MRS has received honoraria for advisory board membership or consultancy from Bristol Myers Squibb, CTI, Forma, Geron, GlaxoSmithKline/Sierra Oncology, Karyopharm, Ryvu Therapeutics, and Taiho Pharmaceutical; has received research funding from ALX Oncology, Astex Pharmaceuticals, Incyte Corporation, Takeda, and TG Therapeutics; holds equity in Empath Biosciences, Karyopharm, and Ryvu Therapeutics; and has been reimbursed for travel expenses by Astex. AK has received honoraria for advisory board membership or consultancy from Geron, Sobi, Incyte Corporation, Morposys, Rigel, and Servier Pharmaceuticals. All other authors have no conflicts of interest to disclose.

Contributions

TM and AGB conceived of the study. TM, YP, and CV processed the targeted sequencing results to call CHIP mutations and germline genetics. TM and YP performed the human genetic association and phenotypic analyses. YP, CAB, and NM performed medications analyses. YL, AK, and YX performed mCA detection. AJ, JVA, and JU performed sequencing of the samples. JBH, AJS, LYL, PBF, AK, and MRS provided important feedback to improve the analysis. TM, YP, and AGB wrote the manuscript with input from all authors. AGB supervised the work. All authors read, revised and approved the manuscript.

Funding

This work was supported by NIH grant DP5 OD029586, a Burroughs Wellcome Fund Career Award for Medical Scientists, an E.P. Evans Foundation grant, a RUNX1 Research Program grant, a Pew Charitable Trusts and Alexander and Margaret Stewart Trust Pew-Stewart Scholar for Cancer Research award, a Vanderbilt University Medical Center Brock Family Endowment grant, and a Young Ambassador award (to AGB); the NHLBI TOPMed eellowship (to TM) NIH grant T32 GM007347 (to YP and AJS); National Institutes of Health grant F30 DK127699 (to AJS); NIH grant K12 CA090625 (to LYL), the Adventure Alle Fund fund, a Beverly and George Rawlings Endowment, and NIH grants R01 CA262287 and U01 OH012271 (to MRS). Research at the Vanderbilt-Ingram Cancer Center is supported by NIH grant P30 CA068485. Vanderbilt University Medical Center's BioVU projects are supported by numerous sources: institutional funding, private agencies, and federal grants. These include NIH funded Shared Instrumentation grant S10OD017985, S10RR025141, and S10OD025092; CTSA grants UL1TR002243, UL1TR000445, and UL1RR024975.

Data-sharing statement

Supplemental table of CHIP mutations and variant allele fractions

is available on GitHub: https://github.com/bicklab/mtp/blob/main/Mack_Pershad_s01.txt. Raw sequencing data will be made available on dbGaP upon publication. Code for the analyses of this paper can be found here: https://github.com/bicklab/mtp. The code to call mosaic chromosomal alterations with MoChA is available here: https://github.com/freeseek/mocha. Code for Mutect2-GATK can be found here: https://gatk.broadinstitute.org/hc/en-us/articles/360037593851-Mutect2. Code to call germline SNP using the targeted assay can be found here: https://github.com/gatk-workflows/gatk4-germline-snps-indels. Code to perform PheWAS analysis can be found here: https://github.com/MASILab/pyPheWAS.

References

1. Bick AG, Weinstock JS, Nandakumar SK, et al. Inherited causes of clonal haematopoiesis in 97,691 whole genomes. Nature. 2020;586(7831):763-768.
2. Jaiswal S, Natarajan P, Silver AJ, et al. Clonal hematopoiesis and risk of atherosclerotic cardiovascular disease. N Engl J Med. 2017;377(2):111-121.
3. Jaiswal S, Fontanillas P, Flannick J, et al. Age-related clonal hematopoiesis associated with adverse outcomes. N Engl J Med. 2014;371(26):2488-2498.
4. Vlasschaert C, Mack T, Heimlich JB, et al. A practical approach to curate clonal hematopoiesis of indeterminate potential in human genetic data sets. Blood. 2023;141(18):2214-2223.
5. Fabre MA, de Almeida JG, Fiorillo E, et al. The longitudinal dynamics and natural history of clonal haematopoiesis. Nature. 2022;606(7913):335-342.
6. Mack T, Vlasschaert C, Von Beck K, et al. Cost-effective and scalable clonal hematopoiesis assay provides insight into clonal dynamics. J Mol Diagn. 2024;26(7):563-573.
7. Uddin MM, Zhou Y, Bick AG, et al. Longitudinal profiling of clonal hematopoiesis provides insight into clonal dynamics. Immun Ageing. 2022;19(1):23.
8. Kessler MD, Damask A, O'Keeffe S, et al. Common and rare variant associations with clonal haematopoiesis phenotypes. Nature. 2022;612(7939):301-309.
9. Weinstock JS, Gopakumar J, Burugula BB, et al. Aberrant activation of TCL1A promotes stem cell expansion in clonal haematopoiesis. Nature. 2023;616(7958):755-763.
10. Wang H, Divaris K, Bohu P, et al. Clonal hematopoiesis driven by mutated DNMT3A promotes inflammatory bone loss. Cell. 2024;187(14):3690-3711.e19.
11. Shannon ML, Heimlich JB, Olson S, et al. Clonal hematopoiesis and inflammation in the VasculaturE (CHIVE): a prospective, longitudinal cohort and biorepository. Blood Adv. 2024;8(13):3453-3463.
12. Díez-Díez M, Ramos-Neble BL, De La Barrera J, et al. Unidirectional association of clonal hematopoiesis with atherosclerosis development. Nat Med. 2024;30(10):2857-2866.
13. Niroula A, Sekar A, Murakami MA, et al. Distinction of lymphoid and myeloid clonal hematopoiesis. Nat Med. 2021;27(11):1921-1927.
14. Weeks LD, Niroula A, Neuberg D, et al. Prediction of risk for myeloid malignancy in clonal hematopoiesis. NEJM Evid. 2023;2(5):10.